

Semi-Supervised Graph Learning Meets Dimensionality Reduction

1st Alex Morehead
Department of EECS
University of Missouri
acmwhb@missouri.edu

1st Watchanan Chantapakul
Department of EECS
University of Missouri
w.chantapakul@missouri.edu

2nd Jianlin Cheng
Department of EECS
University of Missouri
chengji@missouri.edu

Abstract—Semi-supervised learning (SSL) has recently received increased attention from machine learning researchers. By enabling effective propagation of known labels in graph-based deep learning (GDL) algorithms, SSL is poised to become an increasingly used technique in GDL in the coming years. However, there are currently few explorations in the graph-based SSL literature on exploiting classical dimensionality reduction techniques for improved label propagation. In this work, we investigate the use of dimensionality reduction techniques such as PCA, t-SNE, and UMAP to see their effect on the performance of graph neural networks (GNNs) designed for semi-supervised propagation of node labels. Our study makes use of benchmark semi-supervised GDL datasets such as the Cora and Citeseer datasets to allow meaningful comparisons of the representations learned by each algorithm when paired with a dimensionality reduction technique. Our comprehensive benchmarks and clustering visualizations quantitatively and qualitatively demonstrate that, under certain conditions, employing *a priori* and *a posteriori* dimensionality reduction to GNN inputs and outputs, respectively, can simultaneously improve the effectiveness of semi-supervised node label propagation and node clustering. Our source code is freely available on GitHub.

Index Terms—clustering, dimensionality reduction, graph neural networks, semi-supervised learning

I. INTRODUCTION

Semi-supervised learning (SSL), a sub-discipline of unsupervised learning, is focused on transferring information about labeled class samples to unlabeled samples [1]. Recently, semi-supervised learning in the context of graph neural networks (GNNs) has received increased attention by researchers for tasks such as node [2] and graph [3] classification. Under the cluster assumption [1], such efforts, in many common formulations, aim to increase the robustness and accuracy of class clusterings produced on a given dataset through effective propagation of node label information. Concurrently, dimensionality reduction techniques have been widely used throughout several domains in machine learning and other scientific disciplines [4]. Nonetheless, few works have explored the quantitative and qualitative effects of *a priori* and *a posteriori* dimensionality reduction algorithms on the clusterings produced by GNNs, where the dimensionality of each graph’s node representations is reduced before and after a network’s forward pass, respectively. In this

We acknowledge support for this work from two NSF grants, one NIH grant, and three DOE grants. Furthermore, we acknowledge support by the Fullbright program offered through the Thailand-United States Educational Foundation.

work, we explore such effects by investigating the behavior of GNNs for transductive tasks such as semi-supervised node classification on the Cora [5] and Citeseer [6] datasets.

II. RELATED WORK

Few works have explicitly considered leveraging the connection between semi-supervised learning, graph-based learning, and graph-regularized dimensionality reduction to enrich the clustering and classification outputs of GNNs. One of the earliest works on SSL can be found in [7] where authors train Gaussian mixture models to classify text based on labeled and unlabeled documents. Another early work is that of [8], where continuation, a global (non-convex) optimization scheme, is introduced to train semi-supervised support vector machines for image classification across a variety of image datasets. More recently, [9] introduce MixMatch, a deep learning-based approach to SSL on image data. Simultaneously, graph-based deep learning methods have seen a rise in popularity and adoption over the last several years. Notably, works such as those of [10] and [11] demonstrate the effectiveness of GNNs for label propagation in a semi-supervised manner.

In an adjacent way, researchers have developed new methods for dimensionality reduction on manifold datasets [12]. As graphs represent one of many kinds of manifolds, researchers have since applied dimensionality reduction techniques to graph data [13], [14]. Similarly, [15] created a method for learning from graph structures to perform dimensionality reduction in a principled manner. Interestingly, [16] mathematically relate the concepts of graph-regularized PCA to recent developments in graph-based neural networks. Nonetheless, no works have directly and intentionally pursued a comprehensive investigation into the effect of dimensionality reduction algorithms on the inputs and outputs of GNNs. As such, in the proceeding sections, we describe our efforts into elucidating and exploring this idea further, ultimately to determine whether any notable observations or principles may be concretized.

III. METHODS

A. Semi-supervised Learning

Our study employs SSL through the way in which we backpropagate loss through each deep learning model trained. Namely, we mask loss gradients corresponding to unlabeled nodes, where unlabeled nodes are those encountered during

training that were not originally designated to serve in our training dataset. The remainder of our networks’ operations follow conventional deep learning practices [17].

B. Graph Neural Networks

To date, a plethora of GNNs has been developed for SSL on transductive graph datasets. In this work, we explore four deep learning models as methods to perform representation learning or graph message-passing on the Cora and Citeseer datasets. Such models include a multi-layer perceptron (MLP), the Graph Convolutional Network (GCN) [10], the Graph Attention Network (GAT) [18], and the Graph Convolution method (GraphConv) of [19]. First, we let ϕ and ψ represent distinct MLPs, \oplus denote tensor addition, c_{ij} be the edge weight between nodes i and j , and $a(\mathbf{x}_i, \mathbf{x}_j)$ serve as the attention score between nodes i and j . Subsequently, the equations

$$\mathbf{h}_i = \phi(\mathbf{x}_i), \quad (1)$$

$$\mathbf{h}_i = \phi\left(\mathbf{x}_i, \bigoplus_{j \in N_i} c_{ij} \psi(\mathbf{x}_j)\right), \quad (2)$$

$$\mathbf{h}_i = \phi\left(\mathbf{x}_i, \bigoplus_{j \in N_i} a(\mathbf{x}_i, \mathbf{x}_j) \psi(\mathbf{x}_j)\right), \text{ and} \quad (3)$$

$$\mathbf{h}_i = \phi_1(\mathbf{x}_i) + \phi_2\left(\bigoplus_{j \in N_i} c_{ij} \mathbf{x}_j\right) \quad (4)$$

describe how our MLP, GCN, GAT, and GraphConv models, respectively, update with each network layer the current representation \mathbf{x}_i for node i to the updated node representation \mathbf{h}_i . For node classification, after applying a variable number of network layers to our input graphs, we then prepare our graphs’ learned node representations for classification by reducing their dimensionality down to the respective number of node classes in a given dataset using a final chosen network layer.

C. Dimensionality Reduction

When one builds a machine learning model by letting it learn from the data it is provided, one may be convinced that utilizing all available features will be beneficial to the model’s performance and robustness. However, if such features are in a high-dimensional space (e.g., $\vec{x} \in \mathbb{R}^{300}$), this scenario can vividly illustrate the well-known curse of dimensionality that affects how each model behaves. As such, some models may not perform well on higher dimensional data even when they perform well in a lower dimensional space. Fortunately, there are various techniques that we can employ to mitigate the curse of dimensionality. Feature selection methods such as Recursive Feature Elimination (RFE) [20] can be used to do so. Alternatively, one could apply dimensionality reduction techniques as well. These methods directly transform data from a high-dimensional space into a low-dimensional space (e.g., \mathbb{R}^3). The following subsections describe the four dimensionality

reduction algorithms we applied to the inputs or outputs of our chosen GNNs, respectively, to simultaneously reduce input data dimensionality for enhanced semi-supervised node classification performance and to perform robust node-based clustering by visualizing the node representations learned by each semi-supervised GNN after reducing their dimensionality to \mathbb{R}^2 .

1) *Principle Component Analysis*: Principle Component Analysis (PCA)—or Karhunen-Loeve transformation—is one of the most widely used dimensionality reduction techniques since it is an unsupervised algorithm. Invented in 1901 by Pearson [21], PCA operates as follows. Given a vector $\vec{x} \in \mathbb{R}^d$, we define an orthonormal matrix $\mathbf{A} \in \mathbb{R}^{d \times d}$. The matrix-vector multiplication between \mathbf{A} and \vec{x} is then given by

$$\vec{y} = \mathbf{A}^T \vec{x}, \quad (5)$$

a transformation that, once applied to \vec{x} , transforms \vec{x} into \vec{y} in the corresponding new coordinate space. The core idea behind PCA is to preserve the variance of the original data being transformed. Hence, a covariance matrix Σ that represents the covariance between pairs of dimensions plays an important role in PCA. In particular, the eigendecomposition of Σ yields

$$\Sigma \mathbf{A} = \mathbf{A} \Lambda, \quad (6)$$

where \mathbf{A} and Λ are the corresponding eigenvector and eigenvalue matrices, respectively. In the context of PCA, we often keep only the k eigenvectors (denoted as \mathbf{A}_k) that correspond to the k -largest eigenvalues in Λ . In using such results, we get the transformed vector

$$\vec{y}_{k \times 1} = \mathbf{A}_{k \times k}^T \vec{x}_{d \times 1}. \quad (7)$$

Since we normally choose $k \ll d$, this results in a vector in a much lower dimensional space $\vec{y} \in \mathbb{R}^k$. Furthermore, one could set $k = 2$ or $k = 3$. Doing so enables one to plot and visualize the transformed data in \mathbb{R}^2 or \mathbb{R}^3 as such visualizations may be useful for gaining an enhanced intuition regarding the original data’s clustering characteristics.

2) *t-distributed Stochastic Neighbor Embedding*: The t-distributed Stochastic Neighbor Embedding (t-SNE) algorithm [22] has seen wide use by the machine learning community over the last decade [23] for tasks such as visualization of the representations learned by convolutional neural networks. The key equations defining its usage are as follows:

$$p_{ij} = \frac{\exp(-\|x_i - x_j\|^2)/2\sigma^2}{\sum_{k \neq i} \exp(-\|x_i - x_k\|^2)/2\sigma^2}, \quad (8)$$

$$q_{ij} = \frac{(1 + \|y_i + y_j\|^2)^{-1}}{\sum_{k \neq l} (1 + \|y_k - y_l\|^2)^{-1}}. \quad (9)$$

Employing a perplexity of 40 for our datasets, the primary objective of t-SNE is to minimize the Kullback-Leibler (KL) divergence [24] based on the high-dimensional pairwise similarity p_{ij} between point i and point j and the low-dimensional pairwise similarity q_{ij} between point i and point j . Here,

x_i denotes a high-dimensional point, and y_i denotes a low-dimensional point. It can be written in a mathematical form as follows:

$$\min_{y_1, y_2, \dots, y_n} \sum_{i=1}^n \text{KL}(P_i || Q_i) = \min_{y_1, y_2, \dots, y_n} \sum_{i=1}^n \sum_{j=1}^n p_{ij} \log \frac{p_{ij}}{q_{ij}} \quad (10)$$

3) *Uniform Manifold Approximation and Projection*: Since its release in 2018 [25], the Uniform Manifold Approximation and Projection (UMAP) algorithm has been explored with great interest by machine learning researchers as a replacement to t-SNE [26]. It is established upon a representation of a weighted graph. UMAP aims to maintain the local structure and the global structure at the same time after the data is projected down to k -dimensional space through minimizing the cost function which is defined as

$$C_{\text{UMAP}} = \sum_{i \neq j} \underbrace{\left(v_{ij} \log \frac{v_{ij}}{w_{ij}} \right)}_{\text{being neighbors}} + \underbrace{\left((1 - v_{ij}) \log \frac{1 - v_{ij}}{1 - w_{ij}} \right)}_{\text{not being neighbors}}, \quad (11)$$

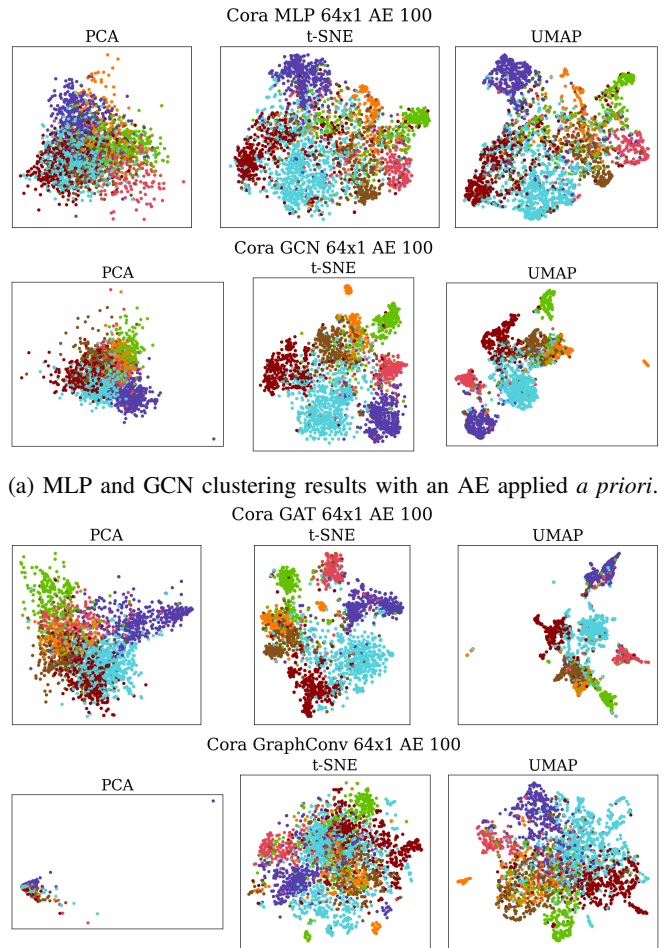
where v_{ij} and w_{ij} are the weights between node i and node j in the high dimensional space and in the low dimensional space, respectively.

4) *Autoencoder*: An autoencoder (AE), as shown in Fig. 3, is another unsupervised learning method for reducing the dimensionality of input data and increasing the robustness of the representations learned by neural networks [27]. It is succinctly comprised of two primary components, an encoder and a decoder. The goal is to find the learned code $\bar{z} \in \mathbb{R}^k$ that best compresses the inputs $\bar{x} \in \mathbb{R}^d$ where $k \ll d$. Notably, during the training phase, for the i -th sample D_i , the output is the same as the input (i.e., $D_i = (\bar{x}, \bar{x})$). Concerning our proceeding experiments, all clustering results obtained by using an autoencoder in an *a priori* manner can be found in Section V-C.

IV. DATA

In this work, we adopt the popular Cora [5] and Citeseer [6] node classification datasets for a series of reasons. First is their wide prior use in the GNN literature on SSL. We also chose these datasets to facilitate a transductive experimentation setting. For graph-based clustering and subsequent visualizations, it is often desirable to narrow focus to a single input graph for training, validation, and testing, which the setting of a transductive dataset directly provides.

The Cora dataset has 2,708 nodes (i.e., samples) and 5,429 edges in total. The number of training samples, validation samples, and test samples, are 140, 500, and 1,000, respectively. Since it has 1,433 unique words in its dictionary, one of its simplest forms of word representation is one-hot encoding. As such, the input features for the Cora dataset are in the set $\mathbb{R}^{1,433}$. The task of this dataset is to classify the subjects of scientific publications. There are seven subjects to be classified: (1) Case Based, (2) Genetic Algorithms, (3) Neural Networks, (4) Probabilistic Methods, (5) Reinforcement Learning, (6) Rule Learning, and (7) Theory.



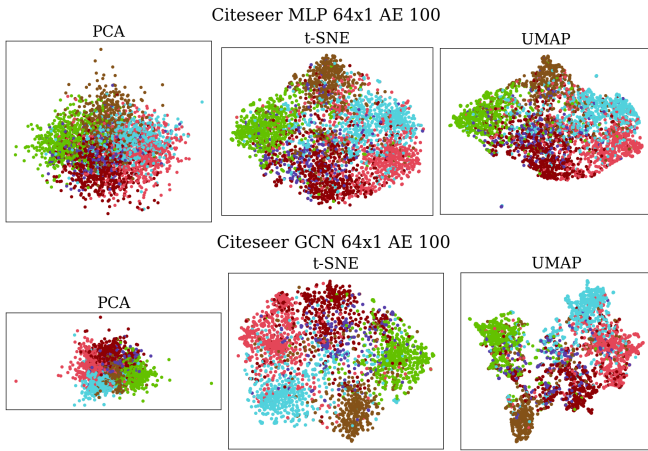
(a) MLP and GCN clustering results with an AE applied *a priori*.

(b) GAT and GraphConv clustering results with an AE applied *a priori*.

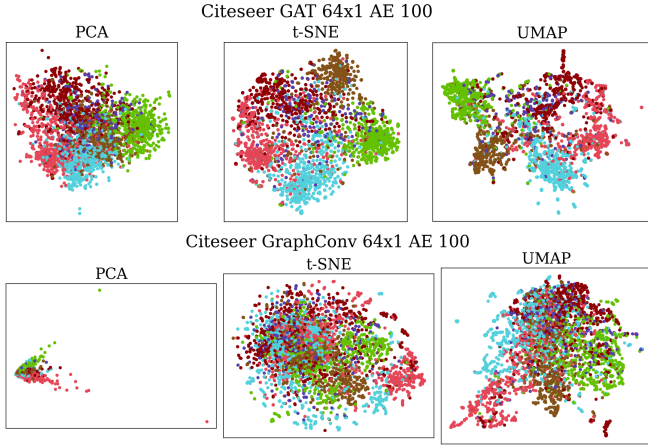
Fig. 1: All models' clustering results on the Cora dataset with an AE applied *a priori*.

Similarly, the Citeseer dataset has 3,327 nodes (i.e., samples) and 9,228 edges in total. It is divided into three subsets, training set (120 samples), validation set (500 samples), and test set (1,000 samples). We utilize one-hot encoding with a size of 3,703 to represent the existence of words in the dataset's publications (i.e., nodes). This dataset also represents a classification problem, but there are now six classes consisting of publications related to (1) Agents, (2) Artificial Intelligence, (3) Database, (4) Information Retrieval, (5) Machine Learning, and (6) Human-Computer Interaction.

From the perspective of graph theory, each Cora publication is a node represented by its encoding in the space $\mathbb{R}^{1,433}$. Likewise, Citeseer uses the space $\mathbb{R}^{3,703}$ to represent its node encodings. This is suitable for GNNs that take graphs as inputs and produce new graphs out. For our semi-supervised study, node classifications on both datasets are performed to get subject predictions as our GNNs' final outputs for each node.



(a) MLP and GCN clustering results with an AE applied *a priori*.



(b) GAT and GraphConv clustering results with an AE applied *a priori*.

Fig. 2: All models’ clustering results on the Citeseer dataset with an AE applied *a priori*.

V. EXPERIMENTS

A. Setup

For all experiments conducted in our study, we used 1 hidden layer of the neural network chosen for the experiment and 64 intermediate channels to restrict the time required to train each model and to prevent the GNN models from

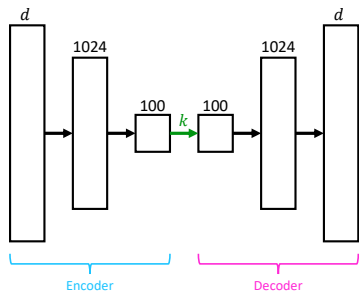
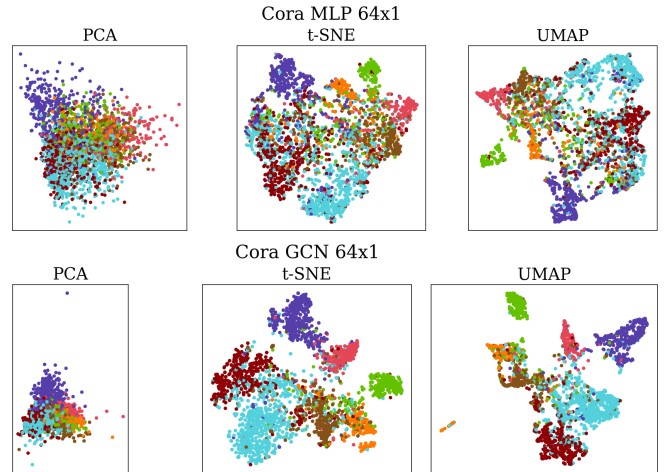


Fig. 3: An outline of our autoencoders’ design

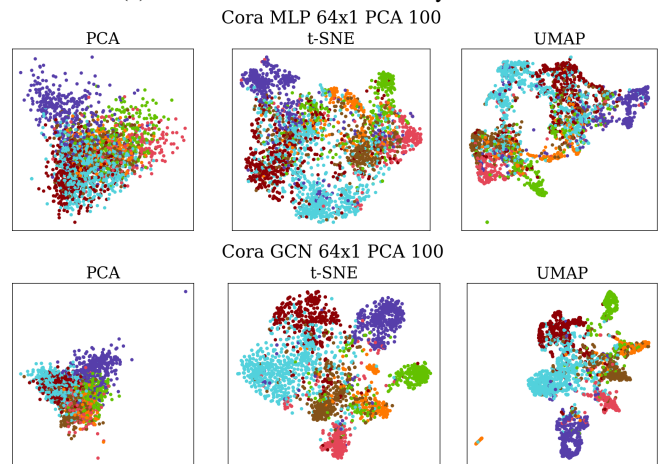
oversmoothing their input node representations [28]. We also arrived at the above configuration after experimenting with increased numbers of hidden layers (e.g., 2) for all models and observing *decreased* classification performance and cluster quality. This means that a GNN with a single layer should be complex enough to solve this problem, for the purposes of our study. Subsequently, we used the stochastic gradient descent (SGD) optimizer [29] with the following, manually-tuned hyperparameters: a learning rate of $1e^{-1}$ (for all models except GraphConv, which required $1e^{-3}$ for training); a weight decay rate of $2e^{-3}$; SGD momentum of 0.9; a dropout (i.e., forget) rate [30] of 0.1; and a batch size of 1. Additionally, with a multi-class cross entropy loss function for backpropagation [31], we employed an early-stopping patience period of 5 epochs based on our validation loss [32].

B. Selection of Autoencoder Bottleneck Size

In the context of training autoencoders, one needs to decide on the size of a bottleneck block to use. Consequently, we chose to validate our choice of bottleneck size by monitoring



(a) Without initial dimensionality reduction



(b) With PCA applied *a priori*

Fig. 4: MLP and GCN clustering results on the Cora dataset.

the mean squared error (MSE) we receive on our datasets' validation partitions with a fixed bottleneck size during the reconstruction of our datasets' original features. Once we identified the bottleneck size with the steepest decline in validation MSE (i.e., 100), which interestingly was the same for both of our datasets, that size became the default for all our experiments with autoencoders.

C. Autoencoder Clustering Visualizations

To explore the use of autoencoders for dimensionality reduction on graphs, we applied them in an *a priori* manner for each dataset during training. Using the node class-color legend illustrated in Fig. 8, based on our analysis Figures 1 and 2 demonstrate that *a priori* autoencoder-driven dimensionality reduction can produce reasonable and interpretable clustering visualizations for both datasets. As a consequence, in Sections V-D and V-E, we see that models trained on features that have had their dimensionality reduced by an autoencoder may also see enhanced clustering quality in quantitative terms. This suggests that exploring dimensionality reduction techniques

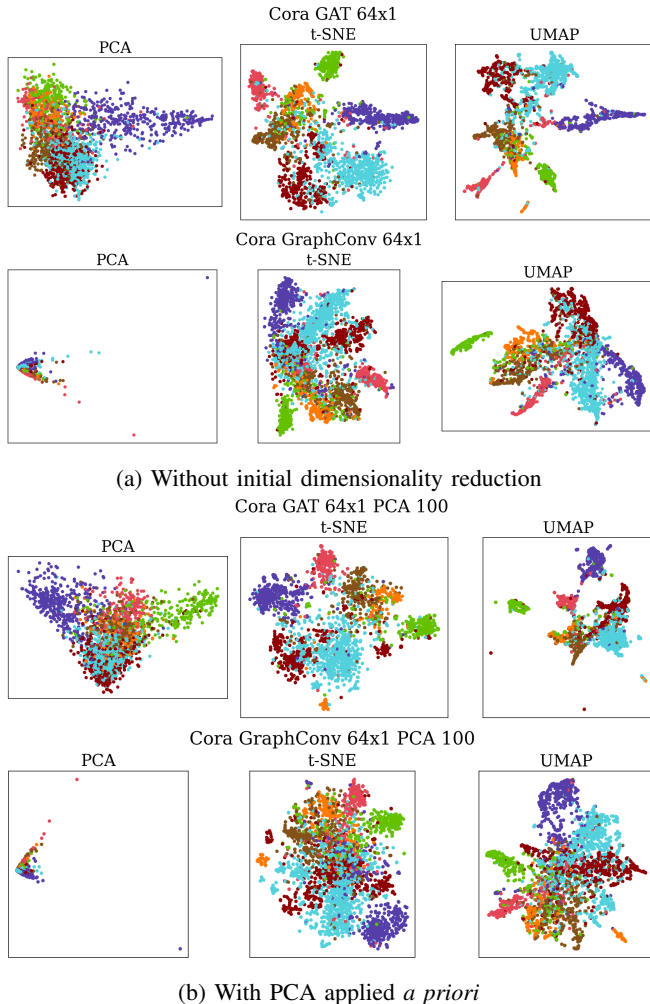


Fig. 5: GAT and GraphConv clustering results on the Cora dataset.

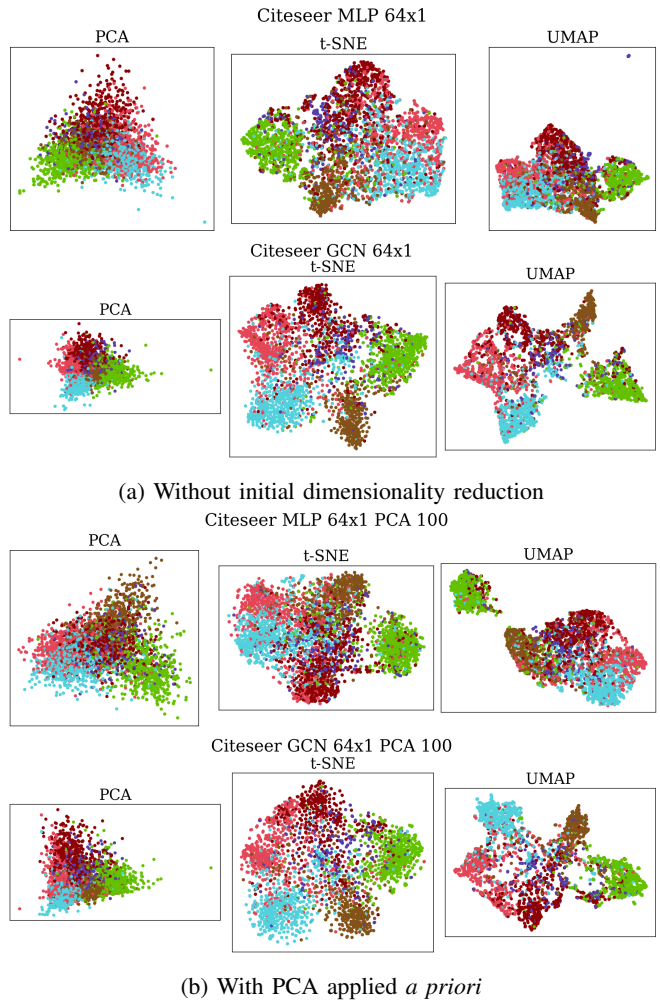


Fig. 6: MLP and GCN clustering results on the Citeseer dataset.

adjacent to autoencoders, namely those specifically designed for graph-based data, may yield improved node clusterings.

D. Cora Results

Table III portrays how for all our selected neural network models except that of [19], applying either PCA or an autoencoder *a priori* favorably achieves low intra-cluster variance and high inter-cluster distance via both the Silhouette Coefficient [33] and the Dunn Index [34]. Particularly interesting to note is that, as Tables I and III show, node clustering and node classification can be seen as complementary tasks. That is, in the context of the Cora dataset, node classification GNNs may improve their classification performance in conjunction with enhancements to their node clustering capability. In summary, we observe that the Cora dataset enables graph neural networks, particularly GCNs, to cluster and classify nodes in a concurrent and performant manner when applying PCA to node features in an *a priori* manner.

E. Citeseer Results

Parallel to our observations in Section V-D, Table IV demonstrates that PCA applied *a priori* to the Citeseer dataset's

TABLE I: The effect of *a priori* dimensionality reduction on node classification for the Cora dataset. Results reported are means and standard deviations (in parentheses) of five separate runs with different random seeds.

Model	Input	Accuracy	Precision	Recall	F1
MLP	Original	58.48 (0.73)	56.08 (0.97)	58.38 (0.64)	56.53 (0.88)
GCN	Original	80.82 (0.62)	79.47 (0.46)	82.21 (0.60)	80.39 (0.57)
GAT	Original	78.36 (0.47)	76.58 (0.65)	79.73 (0.30)	77.68 (0.48)
GraphConv	Original	73.52 (1.52)	72.43 (0.59)	76.27 (1.27)	73.34 (0.96)
MLP	PCA-100	57.90 (1.44)	56.11 (1.76)	58.75 (1.73)	56.46 (1.77)
GCN	PCA-100	80.98 (0.80)	79.77 (0.92)	82.25 (0.70)	80.55 (0.86)
GAT	PCA-100	78.36 (1.39)	77.17 (1.46)	79.78 (1.19)	78.00 (1.31)
GraphConv	PCA-100	72.04 (1.00)	70.79 (0.57)	75.09 (0.99)	72.04 (0.70)
MLP	AE-100	63.24 (0.59)	61.19 (0.61)	63.21 (0.71)	61.72 (0.55)
GCN	AE-100	80.68 (0.45)	78.84 (0.50)	81.57 (0.51)	79.80 (0.45)
GAT	AE-100	77.64 (1.21)	76.11 (0.95)	79.16 (1.15)	77.14 (1.05)
GraphConv	AE-100	60.96 (11.21)	60.01 (12.44)	60.54 (14.63)	58.72 (13.96)

TABLE II: The effect of *a priori* dimensionality reduction on node classification for the Citeseer dataset. Results reported are means and standard deviations (in parentheses) of five separate runs with different random seeds.

Model	Input	Accuracy	Precision	Recall	F1
MLP	Original	56.56 (1.21)	57.85 (0.89)	56.05 (1.09)	55.50 (1.10)
GCN	Original	71.10 (0.84)	68.35 (0.82)	68.67 (0.89)	68.24 (0.86)
GAT	Original	68.84 (0.45)	66.64 (0.43)	66.68 (0.33)	66.15 (0.36)
GraphConv	Original	65.64 (0.85)	63.50 (0.43)	62.83 (0.83)	62.35 (0.75)
MLP	PCA-100	60.60 (0.94)	59.51 (0.73)	58.95 (0.94)	58.59 (0.82)
GCN	PCA-100	70.24 (0.54)	67.65 (0.47)	67.71 (0.46)	67.12 (0.43)
GAT	PCA-100	68.56 (0.84)	65.87 (0.63)	66.03 (0.68)	65.56 (0.73)
GraphConv	PCA-100	63.94 (1.00)	61.41 (0.90)	60.76 (1.15)	60.35 (1.20)
MLP	AE-100	60.60 (1.39)	60.30 (0.94)	59.01 (1.11)	58.61 (1.19)
GCN	AE-100	69.14 (1.50)	66.99 (0.97)	66.83 (1.29)	66.16 (1.37)
GAT	AE-100	67.68 (0.77)	66.19 (0.98)	65.40 (0.90)	64.87 (0.78)
GraphConv	AE-100	45.68 (16.03)	44.71 (18.36)	45.06 (15.48)	42.41 (17.87)

node features results in high quality clusterings. Likewise, we observe in Table II that, although unaltered node features are sufficient for GNNs to achieve our highest observed classification metrics, *a priori* application of PCA enables them to more confidently label document nodes with their respective topics by reducing the variance of their classification performance across different random seeds used for training. As quantitative model confidence measures are desired components of machine learning research, we believe such results illustrate that dimensionality reduction can, in certain settings, reduce the stochasticity associated with the predictions made by GNNs.

F. Model Parameter Efficiency when using Dimensionality Reduction

A tertiary benefit of using dimensionality reduction during model training can come in terms of models’ parameter efficiency. Table V displays the number of learnable parameters for each of our models according to each input feature size. We observe that after applying *a priori* dimensionality reduction techniques to lessen the dimensionality of our datasets’ input features to 100, the number of learnable parameters required for training each of our models is greatly reduced. For the Cora dataset, all models trained with an *a priori* AE or PCA have approximately 13 times fewer trainable parameters compared to training them with Cora’s original input feature size. Concerning the Citeseer dataset, applying dimensionality reduction to our models’ input features decreases their learnable parameter counts by over a factor of 34. Both outcomes represent a noticeable improvement in terms of our models’ size,

computational complexity, and parameter efficiency obtained by applying *a priori* dimensionality reduction.

G. Discussion

We believe there are a few key insights we can distill from our study on dimensionality reduction in the setting of semi-supervised graph learning. Recall that, according to the curse of dimensionality, datasets with samples containing 1,433 and 3,703 dimensions should be considered very high dimensional datasets that are ripe for dimensionality reduction. As a case study for this phenomenon, our visualizations and quantitative results for the Cora dataset suggest that one may want to *a priori* apply either PCA or an autoencoder before using UMAP to visualize learned node features, and reduce the computation time required for training each model. In the context of the Citeseer dataset, we observe a similar trend in that *a priori* dimensionality reduction also positively impacts the node classification and node clustering performance of graph-based neural networks. Nonetheless, employing dimensionality reduction in the setting of graph-based deep learning (particularly semi-supervised graph learning) requires one to consider the underlying characteristics of the dataset being analyzed such as its size and data diversity, as such characteristics may determine whether the use of *a priori* dimensionality reduction is appropriate and desirable.

VI. CONCLUSION

In this work, we have empirically and visually shown that a careful application of *a priori* dimensionality reduction, namely

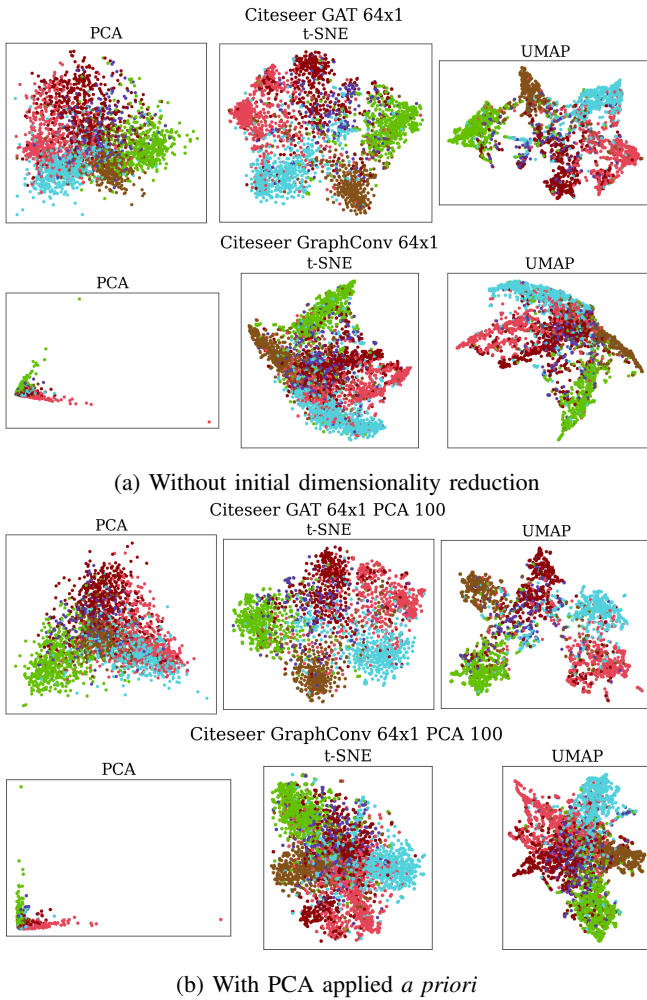


Fig. 7: GAT and GraphConv clustering results on the Citeseer dataset.

Cora:	PM	RL	CB	NN	GA	RLL	Theory
Citeseer:	IR	AI	HCI	Agents	DB	ML	

Fig. 8: Data legend for the Cora dataset and the Citeseer dataset.

autoencoding and PCA, can improve cluster quality and label propagation for enhanced node classification on graph datasets such as Cora while exploring other benefits of dimensionality reduction in GNN-based node clustering. For future work, we believe performing experiments with *a priori* t-SNE and UMAP applied to initial node features may promote further discussions into the characteristics of each dimensionality reduction algorithm for clustering and classification in a graph-transductive setting. Furthermore, we believe expanding the breadth of our study’s transductive graph datasets is likely to yield more insights into how each dataset is best structured for improved pattern recognition. Investigations into alternatives to the autoencoder architecture we used in our study, such as graph variational autoencoders or graph normalizing flows, may provide the groundwork for new studies into advanced GNN-

TABLE III: The effect of *a priori* dimensionality reduction on Cora dataset clusterings. Results reported are taken from the first of our five separate runs.

Model	Input	Output	Silhouette Coefficient	Dunn Index
MLP	Original	PCA	-0.064	37.615
MLP	Original	t-SNE	-0.016	1.831
MLP	Original	UMAP	-0.019	18.202
GCN	Original	PCA	0.012	18.496
GCN	Original	t-SNE	0.212	1.388
GCN	Original	UMAP	0.256	12.407
GAT	Original	PCA	-0.006	27.310
GAT	Original	t-SNE	0.185	1.379
GAT	Original	UMAP	0.200	12.127
GraphConv	Original	PCA	-0.097	3.097
GraphConv	Original	t-SNE	0.047	1.571
GraphConv	Original	UMAP	0.095	15.548
<hr/>				
MLP	PCA-100	PCA	-0.050	37.629
MLP	PCA-100	t-SNE	0.004	1.844
MLP	PCA-100	UMAP	-0.018	14.851
GCN	PCA-100	PCA	-0.013	18.388
GCN	PCA-100	t-SNE	0.195	1.365
GCN	PCA-100	UMAP	0.227	11.888
GAT	PCA-100	PCA	0.048	34.035
GAT	PCA-100	t-SNE	0.154	1.242
GAT	PCA-100	UMAP	0.208	11.649
GraphConv	PCA-100	PCA	-0.111	3.584
GraphConv	PCA-100	t-SNE	0.017	1.597
GraphConv	PCA-100	UMAP	0.043	21.594
<hr/>				
MLP	AE-100	PCA	-0.047	29.394
MLP	AE-100	t-SNE	0.039	1.588
MLP	AE-100	UMAP	0.060	18.739
GCN	AE-100	PCA	0.069	18.208
GCN	AE-100	t-SNE	0.232	1.462
GCN	AE-100	UMAP	0.269	12.372
GAT	AE-100	PCA	0.032	25.572
GAT	AE-100	t-SNE	0.175	1.259
GAT	AE-100	UMAP	0.237	11.019
GraphConv	AE-100	PCA	-0.101	2.023
GraphConv	AE-100	t-SNE	-0.057	1.603
GraphConv	AE-100	UMAP	0.062	23.875

based clustering methods. Finally, we believe that exploring the use of newer graph neural networks for semi-supervised graph learning, networks such as the UniMP and GCNII models, may enrich the contents of future studies and the insights they provide.

REFERENCES

- [1] J. E. Van Engelen and H. H. Hoos, “A survey on semi-supervised learning,” *Machine Learning*, vol. 109, no. 2, pp. 373–440, 2020.
- [2] B. Xu, J. Huang, L. Hou, H. Shen, J. Gao, and X. Cheng, “Label-consistency based graph neural networks for semi-supervised node classification,” in *Proceedings of the 43rd International ACM SIGIR conference on research and development in Information Retrieval*, 2020, pp. 1897–1900.
- [3] Z. Kang, C. Peng, Q. Cheng, X. Liu, X. Peng, Z. Xu, and L. Tian, “Structured graph learning for clustering and semi-supervised classification,” *Pattern Recognition*, vol. 110, p. 107627, 2021.
- [4] G. T. Reddy, M. P. K. Reddy, K. Lakshmana, R. Kaluri, D. S. Rajput, G. Srivastava, and T. Baker, “Analysis of dimensionality reduction techniques on big data,” *IEEE Access*, vol. 8, pp. 54 776–54 788, 2020.
- [5] Q. Lu and L. Getoor, “Link-based classification,” in *Proceedings of the Twentieth International Conference on International Conference on Machine Learning*, ser. ICML’03. AAAI Press, 2003, p. 496–503.
- [6] P. Sen, G. Namata, M. Bilgic, L. Getoor, B. Galligher, and T. Eliassi-Rad, “Collective classification in network data,” *AI magazine*, vol. 29, no. 3, pp. 93–93, 2008.

TABLE IV: The effect of *a priori* dimensionality reduction on Citeseer dataset clusterings. Results reported are taken from the first of our five separate runs.

Model	Input	Output	Silhouette Coefficient	Dunn Index
MLP	Original	PCA	-0.039	46.717
MLP	Original	t-SNE	0.040	1.963
MLP	Original	UMAP	0.053	16.762
GCN	Original	PCA	0.063	27.347
GCN	Original	t-SNE	0.155	1.661
GCN	Original	UMAP	0.162	21.340
GAT	Original	PCA	0.052	49.851
GAT	Original	t-SNE	0.145	1.643
GAT	Original	UMAP	0.169	20.164
GraphConv	Original	PCA	-0.149	4.420
GraphConv	Original	t-SNE	0.071	2.018
GraphConv	Original	UMAP	0.069	22.523
MLP	PCA-100	PCA	-0.008	57.072
MLP	PCA-100	t-SNE	0.054	2.120
MLP	PCA-100	UMAP	0.067	21.253
GCN	PCA-100	PCA	0.042	32.469
GCN	PCA-100	t-SNE	0.154	1.636
GCN	PCA-100	UMAP	0.174	23.572
GAT	PCA-100	PCA	0.016	56.144
GAT	PCA-100	t-SNE	0.141	1.619
GAT	PCA-100	UMAP	0.144	21.416
GraphConv	PCA-100	PCA	-0.150	5.830
GraphConv	PCA-100	t-SNE	0.066	2.107
GraphConv	PCA-100	UMAP	0.114	29.787
MLP	AE-100	PCA	-0.003	34.902
MLP	AE-100	t-SNE	0.072	1.906
MLP	AE-100	UMAP	0.083	25.998
GCN	AE-100	PCA	0.046	22.575
GCN	AE-100	t-SNE	0.146	1.548
GCN	AE-100	UMAP	0.155	24.821
GAT	AE-100	PCA	0.031	37.711
GAT	AE-100	t-SNE	0.143	1.707
GAT	AE-100	UMAP	0.140	21.035
GraphConv	AE-100	PCA	-0.158	3.836
GraphConv	AE-100	t-SNE	-0.089	1.816
GraphConv	AE-100	UMAP	-0.047	30.334

TABLE V: The number of trainable parameters of different combinations of models and inputs.

Model	Input	Number of Trainable Parameters	
		Cora	Citeseer
MLP	Original	23,063	59,366
GCN	Original	23,063	59,366
GAT	Original	23,109	59,410
GraphConv	Original	46,103	118,710
MLP	PCA-100/AE-100	1,735	1,718
GCN	PCA-100/AE-100	1,735	1,718
GAT	PCA-100/AE-100	1,781	1,762
GraphConv	PCA-100/AE-100	3,447	3,414

[7] K. Nigam, A. K. McCallum, S. Thrun, and T. Mitchell, "Text classification from labeled and unlabeled documents using em," *Machine learning*, vol. 39, no. 2, pp. 103–134, 2000.

[8] O. Chapelle, M. Chi, and A. Zien, "A continuation method for semi-supervised svms," in *Proceedings of the 23rd international conference on Machine learning*, 2006, pp. 185–192.

[9] D. Berthelot, N. Carlini, I. Goodfellow, N. Papernot, A. Oliver, and C. Raffel, "Mixmatch: A holistic approach to semi-supervised learning," *arXiv preprint arXiv:1905.02249*, 2019.

[10] T. N. Kipf and M. Welling, "Semi-supervised classification with graph convolutional networks," *CoRR*, vol. abs/1609.02907, 2016. [Online]. Available: <http://arxiv.org/abs/1609.02907>

[11] Z. Yang, W. Cohen, and R. Salakhudinov, "Revisiting semi-supervised learning with graph embeddings," in *International conference on machine learning*. PMLR, 2016, pp. 40–48.

[12] L. Van Der Maaten, E. Postma, J. Van den Herik *et al.*, "Dimensionality reduction: a comparative," *J Mach Learn Res*, vol. 10, no. 66-71, p. 13, 2009.

[13] S. Yan, D. Xu, B. Zhang, H.-J. Zhang, Q. Yang, and S. Lin, "Graph embedding and extensions: A general framework for dimensionality reduction," *IEEE transactions on pattern analysis and machine intelligence*, vol. 29, no. 1, pp. 40–51, 2006.

[14] L. Zhang, S. Chen, and L. Qiao, "Graph optimization for dimensionality reduction with sparsity constraints," *Pattern Recognition*, vol. 45, no. 3, pp. 1205–1210, 2012.

[15] Q. Mao, L. Wang, S. Goodison, and Y. Sun, "Dimensionality reduction via graph structure learning," in *Proceedings of the 21th ACM SIGKDD international conference on knowledge discovery and data mining*, 2015, pp. 765–774.

[16] L. Zhao and L. Akoglu, "Connecting graph convolutional networks and graph-regularized pca," *arXiv preprint arXiv:2006.12294*, 2020.

[17] I. Goodfellow, Y. Bengio, and A. Courville, *Deep learning*. MIT press, 2016.

[18] P. Veličković, G. Cucurull, A. Casanova, A. Romero, P. Lio, and Y. Bengio, "Graph attention networks," *arXiv preprint arXiv:1710.10903*, 2017.

[19] C. Morris, M. Ritzert, M. Fey, W. L. Hamilton, J. E. Lenssen, G. Rattan, and M. Grohe, "Weisfeiler and leman go neural: Higher-order graph neural networks," in *Proceedings of the AAAI Conference on Artificial Intelligence*, vol. 33, no. 01, 2019, pp. 4602–4609.

[20] X.-w. Chen and J. C. Jeong, "Enhanced recursive feature elimination," in *Sixth International Conference on Machine Learning and Applications (ICMLA 2007)*. IEEE, 2007, pp. 429–435.

[21] K. P. F.R.S., "Liii. on lines and planes of closest fit to systems of points in space," *The London, Edinburgh, and Dublin Philosophical Magazine and Journal of Science*, vol. 2, no. 11, pp. 559–572, 1901. [Online]. Available: <https://doi.org/10.1080/14786440109462720>

[22] L. van der Maaten and G. Hinton, "Visualizing data using t-sne," *Journal of Machine Learning Research*, vol. 9, no. 86, pp. 2579–2605, 2008. [Online]. Available: <http://jmlr.org/papers/v9/vandermaaten08a.html>

[23] L. Van der Maaten and G. Hinton, "Visualizing data using t-sne." *Journal of machine learning research*, vol. 9, no. 11, 2008.

[24] T. Van Erven and P. Harremos, "Rényi divergence and kullback-leibler divergence," *IEEE Transactions on Information Theory*, vol. 60, no. 7, pp. 3797–3820, 2014.

[25] L. McInnes, J. Healy, and J. Melville, "Umap: Uniform manifold approximation and projection for dimension reduction," *arXiv preprint arXiv:1802.03426*, 2018.

[26] E. Becht, L. McInnes, J. Healy, C.-A. Dutertre, I. W. Kwok, L. G. Ng, F. Ginhoux, and E. W. Newell, "Dimensionality reduction for visualizing single-cell data using umap," *Nature biotechnology*, vol. 37, no. 1, pp. 38–44, 2019.

[27] A. Ng *et al.*, "Sparse autoencoder," *CS294A Lecture notes*, vol. 72, no. 2011, pp. 1–19, 2011.

[28] D. Chen, Y. Lin, W. Li, P. Li, J. Zhou, and X. Sun, "Measuring and relieving the over-smoothing problem for graph neural networks from the topological view," in *Proceedings of the AAAI Conference on Artificial Intelligence*, vol. 34, no. 04, 2020, pp. 3438–3445.

[29] L. Bottou, "Large-scale machine learning with stochastic gradient descent," in *Proceedings of COMPSTAT'2010*. Springer, 2010, pp. 177–186.

[30] N. Srivastava, G. Hinton, A. Krizhevsky, I. Sutskever, and R. Salakhudinov, "Dropout: a simple way to prevent neural networks from overfitting," *The journal of machine learning research*, vol. 15, no. 1, pp. 1929–1958, 2014.

[31] Z. Zhang and M. R. Sabuncu, "Generalized cross entropy loss for training deep neural networks with noisy labels," in *32nd Conference on Neural Information Processing Systems (NeurIPS)*, 2018.

[32] Y. Yao, L. Rosasco, and A. Caponnetto, "On early stopping in gradient descent learning," *Constructive Approximation*, vol. 26, no. 2, pp. 289–315, 2007.

[33] L. Zhu, B. Ma, and X. Zhao, "Clustering validity analysis based on silhouette coefficient [j]," *Journal of Computer Applications*, vol. 30, no. 2, pp. 139–141, 2010.

[34] C.-E. B. Ncir, A. Hamza, and W. Bouaguel, "Parallel and scalable dunn index for the validation of big data clusters," *Parallel Computing*, vol. 102, p. 102751, 2021.